Influence of simultaneous aging and plasma nitriding on fatigue performance of 17-4 PH stainless steel

Hamidreza Riazi, Fakhreddin Ashrafizadeh, Sayed Rahman Hosseini, R. Ghomashchi

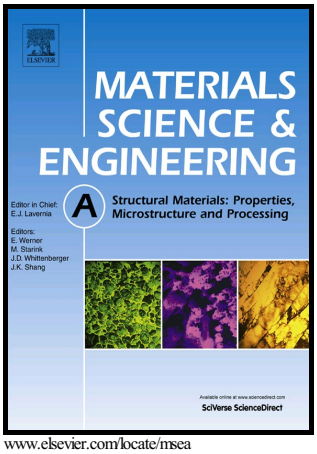

www.elsevier.com/locate/msea

PII: S0921-5093(17)30965-6
DOI: http://dx.doi.org/10.1016/j.msea.2017.07.070
Reference: MSA35318

To appear in: *Materials Science & Engineering A*

Received date: 3 June 2017
Revised date: 30 June 2017
Accepted date: 20 July 2017

Cite this article as: Hamidreza Riazi, Fakhreddin Ashrafizadeh, Sayed Rahma Hosseini and R. Ghomashchi, Influence of simultaneous aging and plasm nitriding on fatigue performance of 17-4 PH stainless steel, *Materials Science Engineering A,* http://dx.doi.org/10.1016/j.msea.2017.07.070

Influence of simultaneous aging and plasma nitriding on fatigue performance of 17-4 PH stainless steel

Hamidreza Riazi[a*], Fakhreddin Ashrafizadeh[a], Sayed Rahman Hosseini[b], R. Ghomashchi[c]

[a]Department of Materials Engineering, Isfahan University of Technology, Isfahan 8415683111, Iran.

[b]Department of Materials Engineering, Maleke-ashtar University of Technology, Isfahan 83145-115, Iran

[c]School of Mechanical Engineering, University of Adelaide, Adelaide, SA 5005, Australia

h.riazi@ma.iut.ac.ir

Website: hriazi.materials.iut.ac.ir

[*]Corresponding autor: Tel.: +983133915714, Fax: +983133912752

ABSTRACT

This paper investigates fatigue behavior of precipitation hardenable 17-4 PH stainless steel after simultaneous aging and plasma nitriding. For this purpose, "solution treated", "aged" and "simultaneous aged and nitrided" specimens were compared in terms of hardness, phase analysis, residual stress and fatigue strength. Hardness values of aged specimens were recorded during aging process to find the optimum condition in terms of time and temperature for plasma nitriding at which specimens can be simultaneously nitrided and aged. Plasma nitrided specimens were analyzed for residual stresses, and its effect on mechanical properties including hardness and fatigue strength. The specimens that were plasma nitrided at lower temperatures had the highest core hardness. Increasing the nitriding temperature/time caused an increase in residual stress and, consequently, a higher surface hardness. Both nitriding and aging processes improved fatigue life by more than 40%. Plasma nitriding imparts beneficial effect mainly during high stress fatigue while aging treatment is more effective on low stress fatigue properties. Specimens nitrided at 500 °C for 5 h experienced longer fatigue life for high stress conditions while specimen aged/nitrided at 400 °C for 10 h exhibited the highest fatigue strength.

Keywords: Stainless steel, 17-4 PH, Fatigue strength, Plasma nitriding, Age hardening.

1. Introduction

17-4 PH (AISI Type 630) alloy is the most well-known precipitation hardening martensitic stainless steels with approximately 3-4 wt. % copper content. The small size copper-rich precipitates distributed within the matrix are responsible for increasing the strength of the steel [1-5]. Due to proper combination of mechanical properties and corrosion resistance in 17-4 PH, applications of this alloy have been extended to a variety of marine constructions, chemical industries and critical components in power plants [4-7].

Although the mechanical properties of this type of steel are generally improved by aging treatment, it is still necessary to increase surface hardness to ensure enhanced wear resistance and higher fatigue performance. Since both wear and fatigue behavior are closely related to the surface characteristics and properties, it is expected that the application of a hard wear resistant surface layer imposing compressive residual stresses would be effective against fatigue and wear failures [8-14].

There are lots of researches related to fatigue performance improvement of 17-4 PH stainless steel by ageing treatments [15-21] and surface modifications such as shot peening [13] and laser transformation hardening [22]. However, there is not many published work in open literature on the simultaneous aging and surface hardening of this alloy and its effect on fatigue behavior.

Nitriding is considered a surface modification process which has different types such as gas nitriding, salt bath nitriding and plasma nitriding. Gas nitriding and salt bath nitriding are not appropriate for surface hardening of stainless steels. This is due to their high treatment temperature at which the core properties of material would deteriorate and corrosion resistance of the alloy could be compromised as a result of chromium depletion, i.e. formation of chromium nitrides [23-29]. In addition, the thin oxide layer on stainless steels resists against the diffusion of nitrogen into the bulk steel (alloy microstructure), thus longer process time may be necessary [30-32]. Therefore, plasma nitriding is used for nitriding of stainless steels due to its lower treatment temperature and removal of oxide layer by argon sputtering [33-38]. It is also believed the heat develops during the plasma nitriding process could accomplish precipitation hardening of the bulk alloy without the risk of overageing phenomena (due to its lower temperature).

Since there is no work on the effect of concurrent plasma nitriding and aging of 17-4 PH, the aim of this study was to improve fatigue behavior of 17-4 PH stainless steel by simultaneous age hardening of the core and plasma nitriding of the surface. It is expected that such treatment would allow both case and core of the material to attain their optimum properties.

2. Experimental procedure

The commercially available 17-4 PH stainless steel used in this study was in the form of hot-rolled and solution-annealed bars. The chemical composition of this alloy is presented in Table 1. Two groups of specimens were prepared from the as-received bars; the first batch was used for aging treatment and determination of the time at which the peak hardness was achieved, as well as for characterization of plasma nitrided layer. These cylindrical specimens were cut from 9.8 mm diameter bars with a height of 10 mm. The second batch of samples was employed for rotating bending fatigue tests; fatigue specimens were machined according to ISO 1143 as shown in Fig. 1 [39]. All specimens were solution heat treated at 1040 °C for 30 minutes, followed by oil quenching and aging treatment at various temperatures.

Table 1 Chemical composition of commercial 17-4 PH stainless steel obtained by optical spectrometry

Element	Cr	Ni	Cu	Mn	Si	Ti+Nb	S	C	P	Fe
wt. %	16.09	4.10	3.10	0.62	0.50	0.189	0.004	0.032	0.029	bal.

Aging temperatures for the first batch of specimens were 400, 420, 440, 460, 480 and 500 ℃, based on precipitation of copper-rich particles and avoiding formation of reverted austenite. Age hardening of the 17-4 PH type stainless steel is mainly attributed to the precipitation of copper-rich phase which begins at about 370 °C [40, 41] and reverted austenite that starts to form above 500 °C [42]. Therefore, the optimum range of aging and plasma nitriding for 17-4 PH was estimated between 400-500 °C at which precipitation of copper occurs while reverted austenite does not form [40-42]. Aging treatment and hardness measurement were continued until the conditions for overaging took place. Four sets of time/temperature were chosen for plasma nitriding process according to the results of aging treatment.

Plasma nitriding of the specimens was carried out using the parameters shown in Table 2. To explore the best set of time/temperature for nitriding process, three temperatures of 400 °C, 450 °C and 500 °C were selected for a duration of 5 h or 10 h. Plasma nitriding was performed in a semi-industrial unit with a 5kW DC power supply. The general sequence of the plasma nitriding experiments comprise sputter cleaning and heating the specimens to 120 ^{o}C in an atmosphere composed of 66 vol. % Ar and 34 vol. % H_2. A third of gas mixture is hydrogen due to its anti-oxidizing properties to prevent any oxide formation on the surface during sputter cleaning process. Sputter cleaning was carried out at 40 Pa (0.3 Torr) pressure of H_2-Ar mixture for approximately 10 min, after which the heating cycle was started. Upon reaching the prescribed temperature, the atmosphere was switched to a mixture of 75 vol. % H_2 and 25 vol. % N_2 and the nitriding cycle began; total gas pressure was kept at about 400 Pa (3 Torr) in all tests. Adding hydrogen to the gas mixture is due to decrease activity of nitrogen in gas mixture to prevent any chromium nitride formation in the nitrided layer. After the nitriding cycle completed, the power supply was switched off and the specimens were allowed to cool down in the furnace under vacuum to obtain a moderate cooling condition. Specimens were removed from the chamber at room temperature.

Table 2 Nitriding conditions and parameters

Parameters	process designation	Temp. (^{o}C)	Time (h)	Pressure (Pa,Torr)	Gas mixture ratio
Sputter cleaning	Pretreatment for all nitrided specimens	120	0.5	40, 0.3	Ar / H_2 = 2
Plasma nitriding	PN400C5h	400	5	667, 5	H_2/N_2 = 3
	PN400C10h	400	10	667, 5	H_2/N_2 = 3
	PN450C5h	450	5	667, 5	H_2/N_2 = 3
	PN500C5h	500	5	667, 5	H_2/N_2 = 3

For rotating bending fatigue specimens, two sets of plasma nitriding parameters were chosen based on the highest hardness values obtained in aging process and the optimum condition attained in nitriding process. These two plasma nitrided fatigue specimens were, then, compared with their corresponding fatigue specimens at aged condition and solution annealed condition. Surface of all specimens were polished to achieve a fine surface finish (Ra = 0.1 μm).

Before nitriding, the material was pre-cleaned by ultrasonic in acetone bath for 20 minutes at 30 ^{o}C and dried.

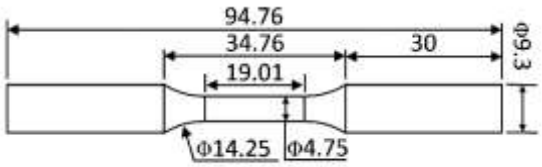

Fig. 1 Rotating bending fatigue specimen dimensions (mm) according to ISO 1143 [39].

Hardness measurements on the surface of specimens were taken on a Rockwell Hardness tester using a load of 1471 N (150 kgf). Rockwell C hardness measurement of each specimen was performed during aging at specific time intervals until overaging took place. The hardness data fitted by MATLAB programming in order to find the exact time for aged condition and time taken for aging at the specific temperature. Microhardness values were also measured by a Vickers mini-load hardness tester with dwell time of 10 s under 0.24 N (25 gf) load.

X-ray diffraction (XRD) analyses were performed by a PHILIPS X'Pert diffractometer connected to a generator at 40 kV and 30 mA with Cu-Kα radiation, wavelength of 1.54439 Å, at a scan rate of 0.01 degree per second. A FEI Quanta 450 FEG-SEM scanning electron microscope was used to study fatigue fracture surface and cross sections of nitrided specimens which were polished and etched with Kalling's [5 g $CuCl_2$, 100 ml HCl (37% conc.) and 100 ml ethanol (96% conc.)] etchant solution [43]. For fractography of fatigue surfaces, the samples were slightly tilted to make striations and beach marks more visible.

Residual stress measurements of nitrided specimens were performed on a PHILIPS X'Pert X-ray Diffractometer (XRD) using Cu-Kα operating at 40 kV and 40 mA under $\sin^2\psi$ method. Scanning were done on $44.674^{o}\pm2$ 2θ peak of martensite which is related to (110) plane. Maximum of peaks at different ψ (psi) values were determined by the Pearson VII fitting method and residual stresses were evaluated from slope of d-spacing vs. $\sin^2\psi$ diagram. The measurement procedures followed are documented in the practice guide published by Fitzpatrick et al. [44].

Fatigue tests were conducted using a four point rotating bending fatigue test machine (SFT-850 SANTAM Co.) under applied frequency of 50 Hz and stress ratio of R= -1. Fatigue strength was assumed to be the stress value at which specimen continues to rotate more than 10^7 cycles without failure. Since it fits the results with the maximum regression, a 5-parameters exponential decay function was used for fitting rather than Weibull, rational function or other common functions used for decay.

3. Results and discussion

3.1 Aging treatment of 17-4 PH steel

Measured values of Rockwell hardness of 17-4 PH specimens after aging process at various time intervals for each temperature are shown in Figure 2. The maximum hardness value of the fitted curves along with the optimum time of aging at specific temperature are presented in Table 3. Decaying wave function was used for fitting age hardening results to show a decay to reach a constant value after having a maximum. The curves start from hardness value for the solution annealed condition, i.e. 31 HRC. It is evident that the higher the temperature, the shorter is the time to reach the maximum hardness. On the other hand, the higher the temperature, the lower is the peak hardness. The time required of aging to obtain maximum hardness increased from 20 minutes at 500 ˚C to 10 hours at 400 ˚C; the surface hardness raised from 41 HRC at 500℃ to 45 HRC at 400 ℃. According to these results and considering the range of temperatures normally used for plasma nitriding of stainless steels, the temperature/time set of 400 ^{o}C/10h is more appropriate for nitriding process to get the higher hardness of the core beneath the nitrided layer, regardless of surface hardness of nitrided specimens which is explained in the next section.

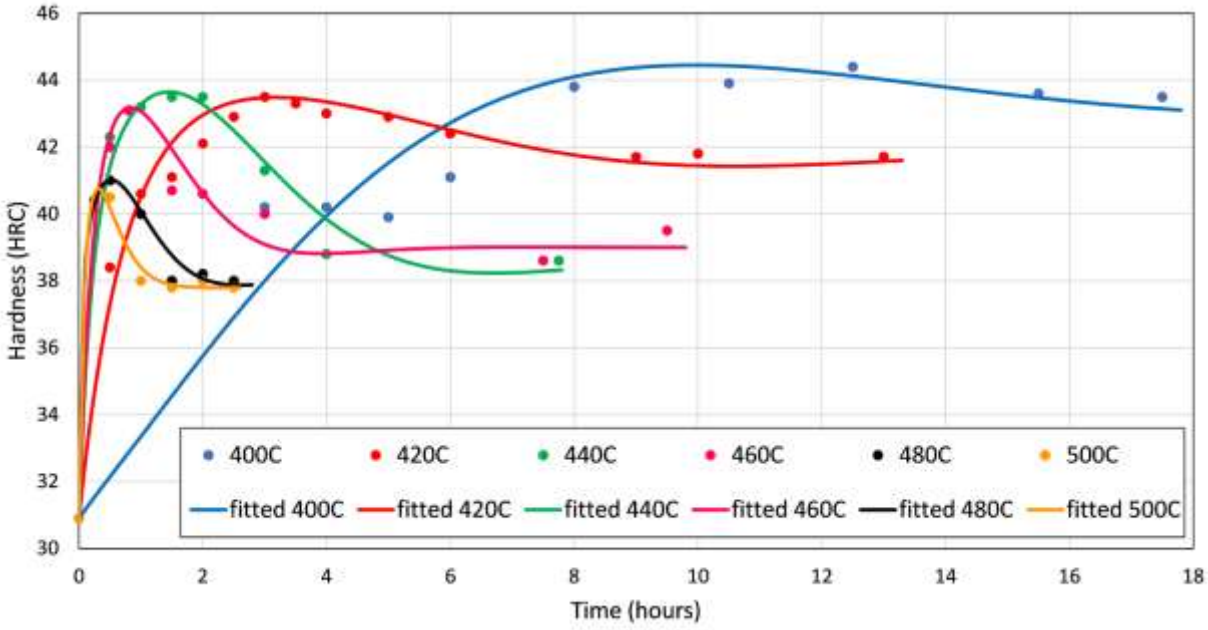

Figure 2 Variation in hardness of 17-4PH stainless steel versus aging time at different temperatures.

Table 3 Maximum Rockwell C hardness and optimum time of aging at various temperatures

Temperature (^{o}C)	400	420	440	460	480	500
Time (hour)	10	3	1.5	0.8	0.5	0.33
Max. Hardness (RC)	45	44	44	43	41	41

3.2 Results of plasma nitriding

X-ray diffraction patterns of solution treated 17-4 PH steel along with nitrided specimens are presented in Figure 3. As can be seen, the main diffraction peaks belong to martensite phase (assigned as M) with their FWHMs (full width at half maximum) increasing after nitriding. The

d-spacing of the nitrided martensite has become approximately 0.7% larger when compared to the solution treated stainless steel (d-spacing of (110) planes for solution treated specimen was 2.036 Å and that of PN4005h was 2.059 Å) indicating the formation of expanded martensite phase; the peaks are assigned as EM. For specimens nitrided at higher temperatures, i.e. 450 ˚C and 500 ˚C, Fe_3N and Fe_4N formed in addition to the expanded martensite phase. Also there are some traces of CrN in the patterns of nitriding at higher temperatures. Diffraction peaks for the base steel (17-4 PH) are not distinct in the XRD patterns for specimens nitrided at temperatures of 450 and 500 ˚C, confirming that the diffusion layer was sufficiently thick to prevent penetration of X-rays into the substrate. Effective depth of penetration for X-rays in 17-4 PH is about 8μm [45].

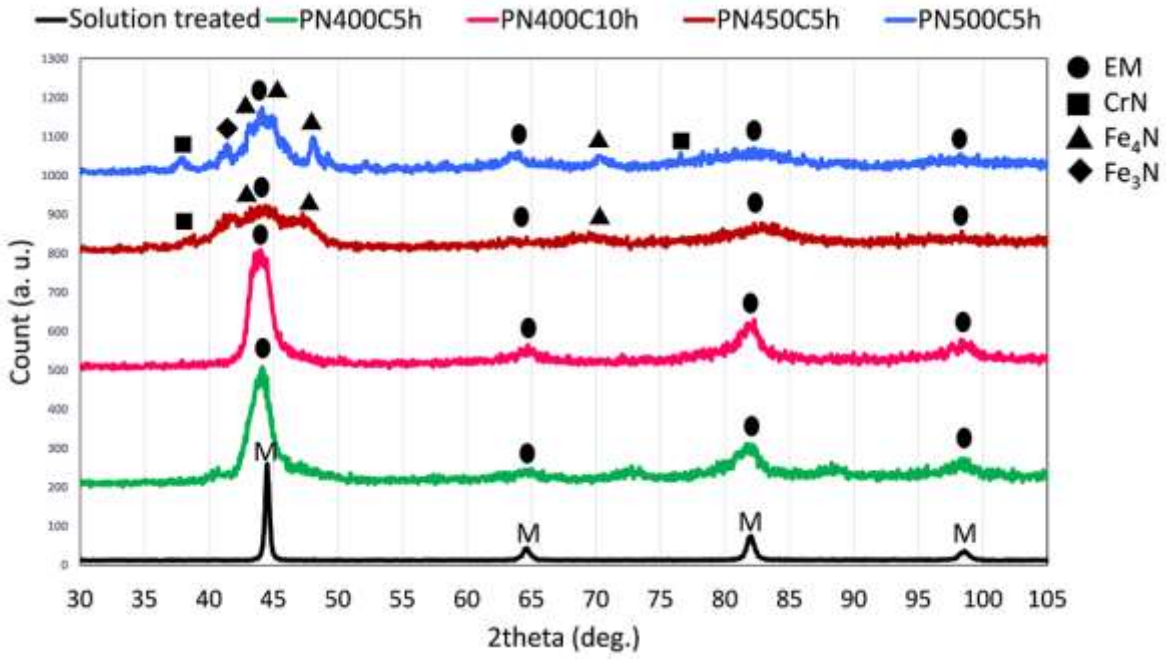

Figure 3 XRD patterns of untreated and plasma nitrided 17-4 PH at different conditions.

SEM micrographs from cross sectional view of the plasma nitrided specimens at different temperatures are shown in Figure 4. As can be seen, the higher the nitriding temperature, the thicker is the nitrided layer. The thickness of nitrided layer increases from about 2.5 μm to nearly 4, 11 and 23 μm for PN400C10h, PN450C5h and PN500C5h, respectively. As expected, for specimens treated at 400 °C, there is no significant enlargement in layer thickness with increasing process time; confirming greater dependency of nitrogen diffusion on temperature than time.

For specimens which were nitrided at 400 °C, the compound layer did not etch by Kalling's reagent, whereas the layer was lightly etched at 450 °C. At 500 °C, it was completely etched before the substrate became etched. This could be due to precipitation of CrN in the compound layer at higher temperatures (Figure 4) that caused formation of chromium depleted regions near the grain boundaries, thus making them more susceptible to corrosion.

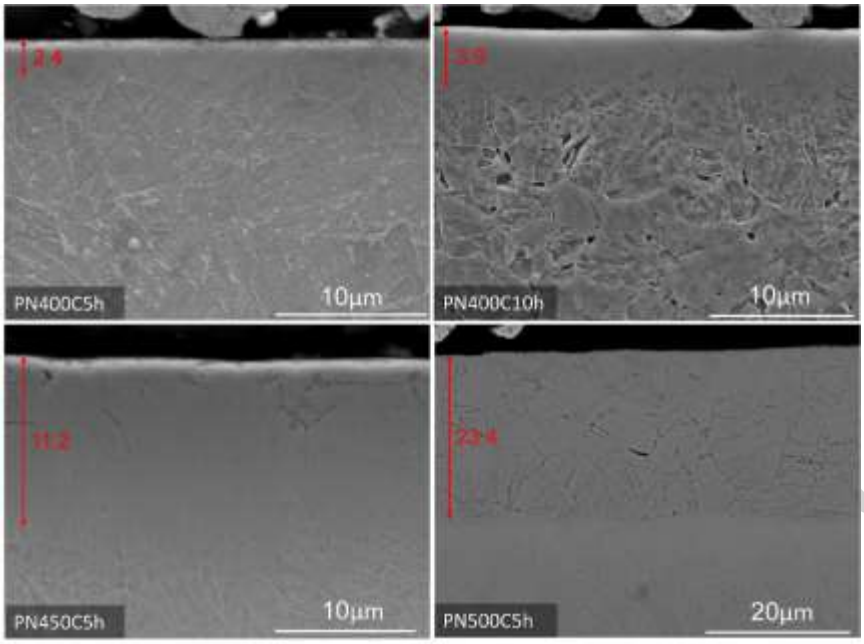

Figure 4 Cross sectional SEM micrographs of plasma nitrided 17-4 PH stainless steel at different temperatures and times.

Values of surface hardness and core hardness for plasma nitrided specimens at different conditions are shown by the bar chart of Figure 5. Higher surface hardness corresponds to specimen PN500C5h which had thicker nitrided layer compared to other nitrided specimens. The measured hardness on the surface of this specimen was approximately 5 times higher than substrate hardness. These data reveal that all nitrided specimens were aged during plasma nitriding process; the core hardness of all specimens is higher than the hardness of solution treated steel, i.e. 310 HV.

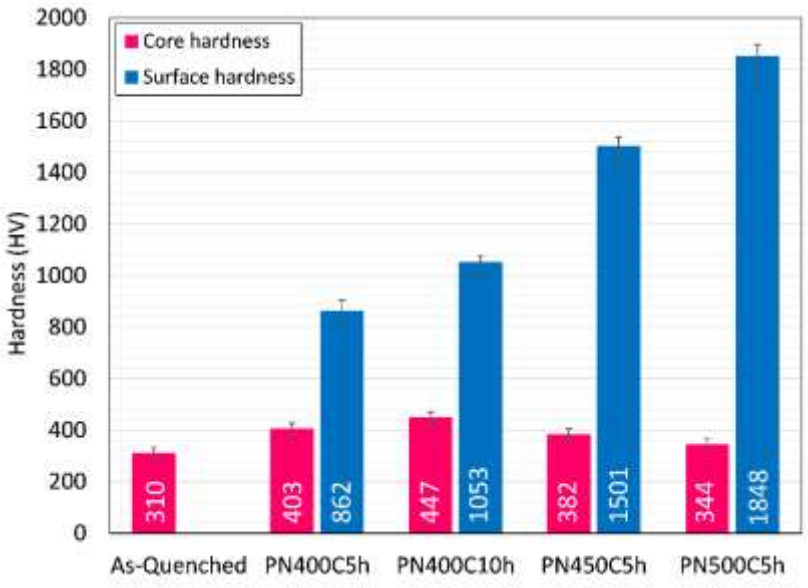

Figure 5 Core and surface hardness values of plasma nitrided 17-4 PH in comparison to solution annealed and quenched specimen.

Figure 6 compares the values of residual stress as measured on typical nitrided specimens. All measurements revealed the development of compressive residual stress on the surface due to diffusion of nitrogen as interstitial atoms. Compressive residual stress in PN400C5h (~ -550 MPa) was lower than those of other three plasma nitriding conditions (~ -850 MPa) which is due to lower diffusion of nitrogen at lower temperature and shorter time of nitriding process. On the other hand, residual stress did not change significantly in PN400C10h, PN450C5h and PN500C5h. This effect may be attributed to two factors that act in opposite directions; one is increasing of residual stress by the extent of diffused nitrogen atoms and the second is decreasing residual stress by stress relaxation, both increase by temperature. The final residual stress would be the net effect of these two factors. Although measured compressive residual stresses are high compared to the results of Raman et al. [46] (-195 MPa for residual stress of plasma nitrided AISI 304 stainless at 460 ^{o}C for 6 h), it is in the range of value reported by Xi et al. [36] (-617 MPa for residual stress of plasma nitrided AISI 420 stainless steel at 350 ^{o}C for 15 h). However these hardness values are much lower than those reported elsewhere; as high as 1-3 GPa in compressive mode [9, 47-50]. High values of compressive residual stresses can improve fatigue resistance of components by suppressing fatigue crack initiation and its propagation. Based on the results reported here, the best nitriding temperature and time to get thicker nitrided layer, optimum hardness and higher compressive residual stress are 500 ^{o}C and 5h, respectively.

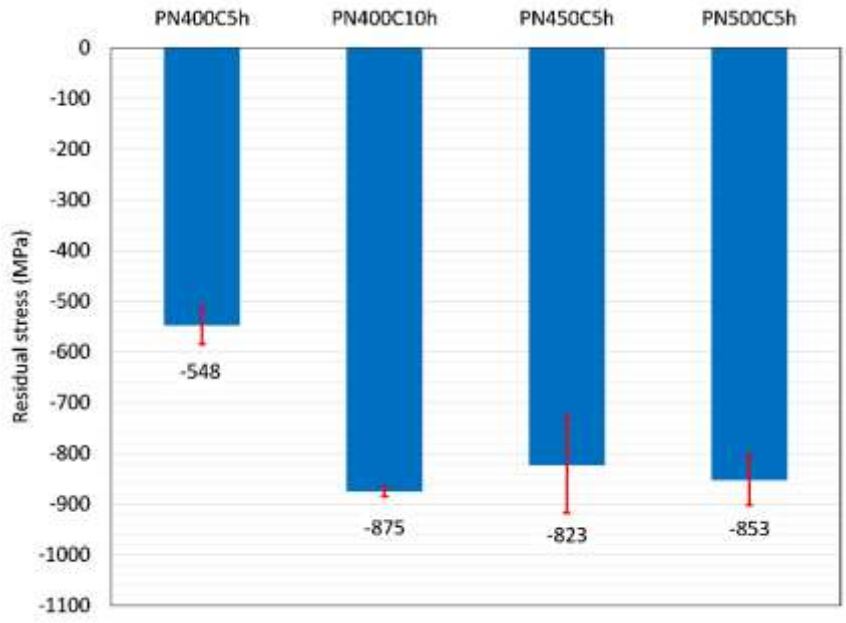

Figure 6 Residual stress values at surface of plasma nitrided specimens at different conditions.

3.3 Fatigue behavior

Based on the results of aging treatment (Figure 2) and characterization of plasma nitrided layer, specimen PN400C10h with maximum core hardness and specimen PN500C5h with optimum surface properties were selected for rotating bending fatigue tests. To investigate the effect of plasma nitriding on fatigue behavior of 17-4PH stainless steel, nitrided specimens should be compared with those heat treated under the same time/temperature condition. For overall comparison, five sets of specimens were selected for fatigue testing; S-N curves for these five conditions are presented in Figure 7.

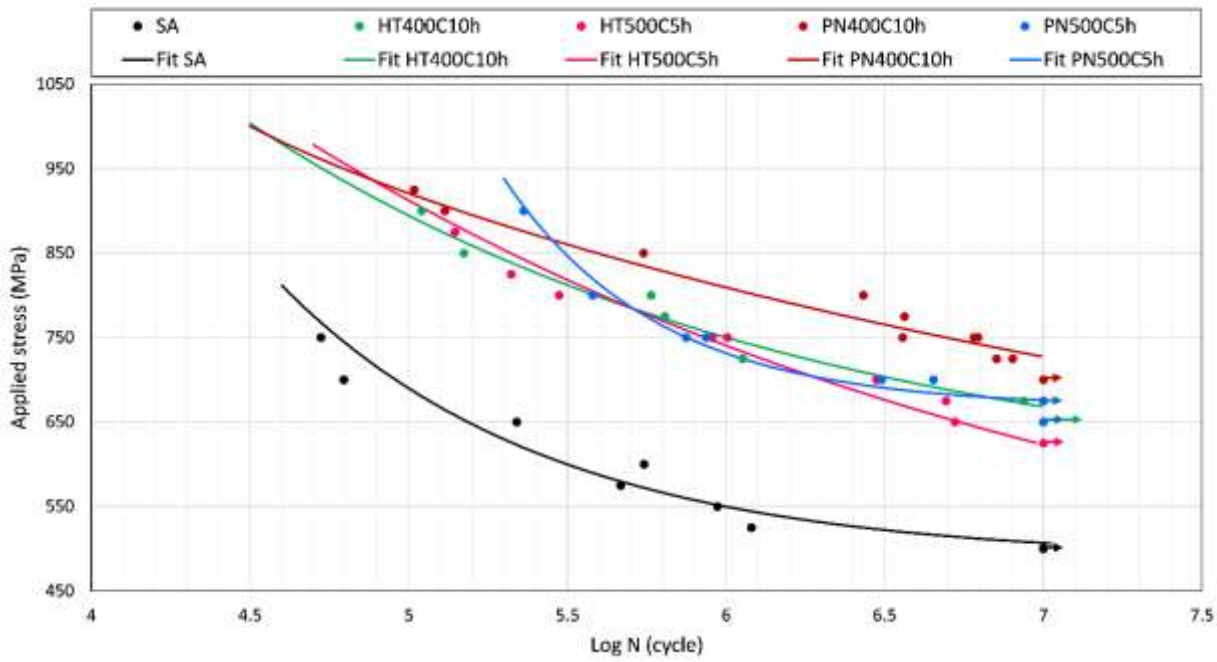

Fig. 7 S-N curves of solution annealed, heat treated and plasma nitrided 17-4 PH.

It is evident from Figure 7 that fatigue strength and fatigue life of solution annealed 17-4 PH are significantly lower than those of treated specimens. Fatigue strength of the specimens in all test conditions are listed in Table 4. Fatigue strength for solution annealed specimens was nearly 500 MPa, more than 100 MPa less than the treated specimens. In other words, aging and plasma nitriding increase the resistance of 17-4 PH stainless steel against fatigue failure by 23-44%.

Table 4 Fatigue strength of solution annealed, heat treated and plasma nitrided 17-4 PH

Specimen condition	Solution annealed	HT400C10h	HT500C5h	PN400C10h	PN500C5h
Fatigue strength (MPa)	506 ± 16	668 ± 22	625 ± 11	727 ± 39	675 ± 26

For interpretation of S-N curves, three types of comparison may be applied. First, comparison of two plasma nitrided conditions; second, comparison of two heat treatment conditions; and third, comparison of each plasma nitrided condition with its corresponding heat treatment condition.

Comparison between S-N curves of plasma nitrided specimens shows that, in higher stress, high temperature nitrided specimens possess optimum fatigue life, whilst in lower stress, low temperature nitrided specimens have better performance. For interpretation of the results, fatigue curves were assumed to be composed of two parts of high stress fatigue (HSF) region and low stress fatigue (LSF) region. In HSF, the major part of fatigue life corresponds to fatigue crack nucleation; after nucleation, it will grow rapidly until sudden fracture occurs. On the other hand, in LSF, fatigue crack propagation takes more time than its nucleation. Since the thickness of hard nitrided case in PN500C5h is 6 times thicker than that of PN400C10h, also their residual stresses are approximately equal, crack nucleation on the surface of PN500C5h is more difficult than PN400C10h. Therefore, fatigue life of PN500C5h in high stress fatigue region is higher. But, in low stress fatigue region, noting that core properties of PN400C10h, where fatigue crack

propagates (Figure 8), is better than that of PN500C5h, fatigue crack growth of low temperature nitrided specimens is more difficult than crack growth in high temperature nitrided specimens. Therefore, fatigue strength of PN400C10h is 8 % higher than that of PN500C5h.

It is the same for comparison of S-N curves of heat treated specimens. In high stress fatigue region, since surface quality of HT400C10h was as smooth as HT500C5h, fatigue life of both specimens became approximately equal. As it is evident in Figure 7, in high stress fatigue region, S-N curves for heat treated specimens are overlapped. In contrast, in low stress fatigue region, specimen HT400C10h is in the aged condition with maximum hardness and strength, and its fatigue strength is 7 % higher than that of HT500C5h.

For investigation of the effect of surface treatment on fatigue behavior of 17-4 PH stainless steel, plasma nitrided specimens were compared with those heat treated under identical conditions; specimens that were heat treated or plasma nitrided at 400 ^{o}C for 10 h. Plasma nitrided specimens presented better fatigue life in both HSF and LSF regions. In high stress fatigue region where surface properties controls the fatigue behavior, plasma nitrided specimen have higher fatigue life due to higher compressive residual stress on the surface (-875 MPa) and higher hardness value (1053 HV) as compared to heat treated specimens. On the other hand, in low stress fatigue region, core properties of both specimens are the same; therefore, what controls the fatigue properties is the surface quality which is superior in PN400C10h. S-N curve of plasma nitrided specimens is above that of heat treated specimens; plasma nitriding at 400 ^{o}C increased the fatigue strength of 17-4 PH stainless steel by 9% from 668 MPa to 727 MPa.

The situation is the same for PN500C5h and HT500C5h; i.e. in both high stress and low stress fatigue regions, plasma nitrided specimens showed more resistance to fatigue failure. In high stress fatigue region, since initiation of cracks depends upon the surface properties, plasma nitrided specimens with high surface hardness, high compressive residual stress on the surface and a thick nitrided layer of about 23 μm, endure more against fatigue failure. In low stress fatigue region, where core properties control fatigue resistance of the material, again PN500C5h showed higher fatigue strength than HT500C5h. Since their core properties are the same, due to similar heat treatment parameters, the difference between their fatigue strengths must be due to different surface properties.

3-4 Fatigue fractography

It is well established that fatigue fracture appearance has three major parts; crack initiation site, crack propagation region and final rupture. Figure 8 shows crack initiation site of heat treated and plasma nitrided specimens. In heat treated condition, crack is nucleated from the surface at which the applied stress is highest during rotating- bending motion. On the other hand, crack nucleation site in plasma nitrided fatigue specimens is not visible since it is beneath the compound layer. A hard nitrided skin on the surface, with high compressive residual stress, covers all around the fatigue specimen, suppressing the crack initiation site on the surface; maximum stress is transferred below the surface, then, crack would initiate and propagate from the substrate [31].

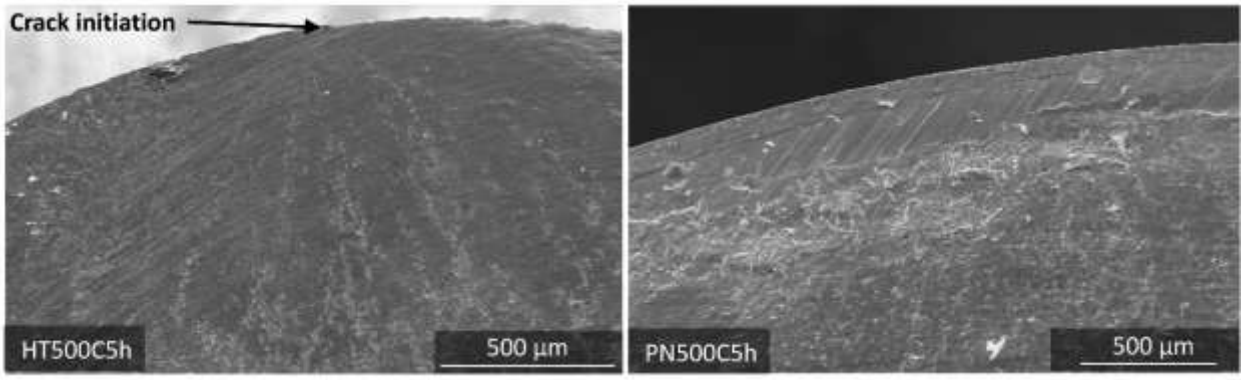

Figure 8 Crack initiation and propagation in heat treated (HT500C5h) and plasma nitrided (PN500C5h) 17-4 PH.

Crack propagation region in rotation bending fatigue fracture surface of 17-4 PH stainless steel showed three types of markings. As it can be seen in Figure 9, depending on light direction of stereo-microscope, beach marks (Figure 9a) or river pattern (Figure 9b) can be observed on the fracture surface; this was true for all specimens. In higher magnification, striations can be seen perpendicular to the beach marks and parallel to the river marks (Figure 10a). Distance between striations were from micro to nano order of magnitude (Figure 10b). It confirms that crack nuclei grew through the center and then propagated toward periphery of the specimen. Beach marks are due to first propagation of crack through the center and striations are due to propagation radially toward outer surface of specimen.

Final fracture appearance of all specimens, untreated and treated, were the same; they finally fractured in ductile mode as it is typically presented in Figure 11.

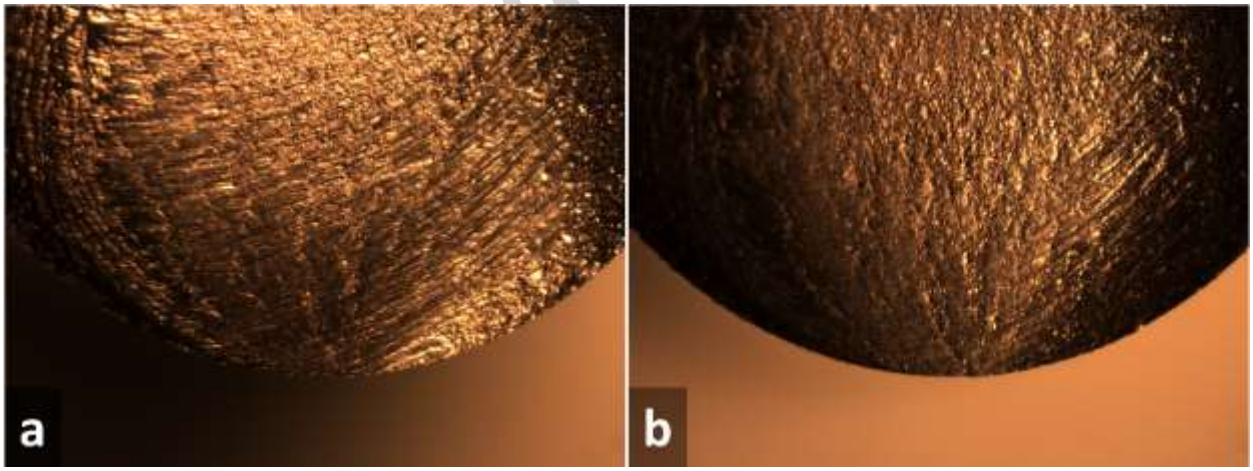

Figure 9 Appearance of fatigue fracture surface with two different direction of light exposure; a) from top, b) from right.

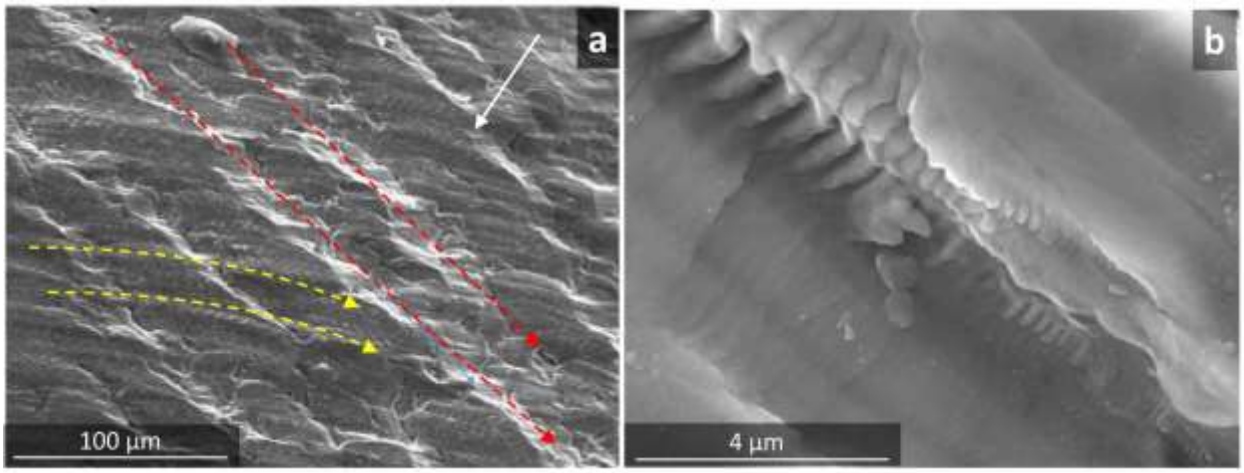

Figure 10 Fatigue fracture surface; a) yellow arrows: beach marks, red arrows: river marks, white arrow: striations, b) striations.

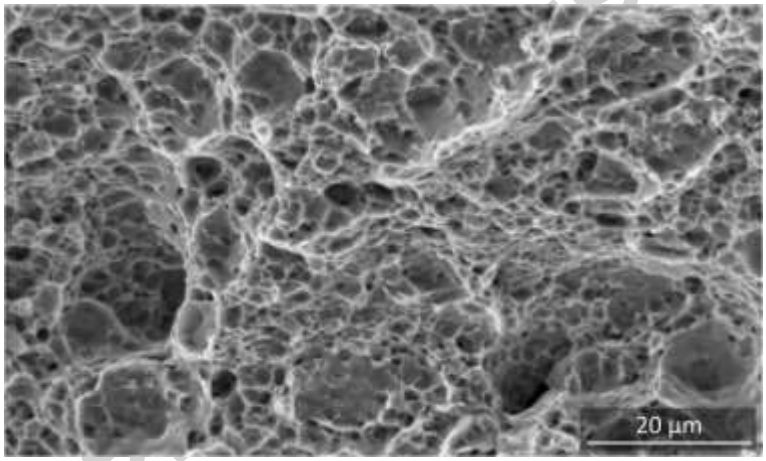

Figure 11 SEM micrograph of final fatigue fracture of 17-4 PH stainless steel.

4. Conclusions

1- At low temperature plasma nitriding (400 ˚C), expanded martensite was the only phase detected on the surface of 17-4 PH steel. At higher process temperatures (450 ˚C and 500 ˚C) nitride phases such as CrN, Fe_3N and Fe_4N were formed.

2- Residual stress on plasma nitrided surface was dependent on temperature, time and amount of nitrogen diffused during nitriding process. Higher temperature and longer time increase the amount of diffused nitrogen atoms, leading to more compressive residual stress, at the same time, it can temper the test piece and make residual stress released.

3- Both aging and plasma nitriding improve fatigue behavior of 17-4 PH up to 44 %; simultaneous nitriding and aging produce the optimum improvement in fatigue performance.

4- High stress fatigue is more dependent on the surface properties of specimens, whereas low stress fatigue can be more controlled by core properties of the alloy.

5- Fatigue crack is initiated from the surface of specimens in the aged conditions and it is nucleated from beneath the nitrided layer after plasma nitriding process.

5. Acknowledgment

The authors would like to thank Isfahan University of Technology-Iran for its financial support and provision of research facilities, Maleke Ashtar University of Technology-Iran for plasma nitriding services, and Adelaide microscopy, University of Adelaide-Australia for technical supports and electron microscope facilities.

References

[1] M. Murayama, K. Hono, and Y. Katayama, "Microstructural evolution in a 17-4 PH stainless steel after aging at 400 C," *Metallurgical and Materials Transactions A*, vol. 30, pp. 345-353, 1999.

[2] U. Viswanathan, S. Banerjee, and R. Krishnan, "Effects of aging on the microstructure of 17-4 PH stainless steel," *Materials Science and Engineering: A*, vol. 104, pp. 181-189, 1988.

[3] J. Wang, H. Zou, C. Li, R. Zuo, S. Qiu, and B. Shen, "Relationship of microstructure transformation and hardening behavior of type 17-4 PH stainless steel," *Journal of University of Science and Technology Beijing, Mineral, Metallurgy, Material*, vol. 13, pp. 235-239, 2006.

[4] J. Wang, H. Zou, C. Li, S. Qiu, and B. Shen, "The spinodal decomposition in 17-4PH stainless steel subjected to long-term aging at 350° C," *Materials Characterization*, vol. 59, pp. 587-591, 2008.

[5] C. Hsiao, C. Chiou, and J. Yang, "Aging reactions in a 17-4 PH stainless steel," *Materials Chemistry and Physics*, vol. 74, pp. 134-142, 2002.

[6] J.-H. Wu and C.-K. Lin, "Influence of frequency on high-temperature fatigue behavior of 17-4 PH stainless steels," *Materials Transactions*, vol. 44, pp. 713-721, 2003.

[7] W. Jun, Z. Hong, W. Xiao-yong, L. Cong, Q. Shao-yu, and S. Bao-luo, "The Effect of Long-Term Isothermal Aging on Dynamic Fracture Toughness of Type 17-4 PH SS at 350. DEG. C," *Materials transactions*, vol. 46, pp. 846-851, 2005.

[8] G. Minak, "on the improvement of the fatigue behaviour of austenitic stainless steels due to surface residual stresses produced by low temperature carburizing."

[9] S. Kikuchi, Y. Nakahara, and J. Komotori, "Fatigue properties of gas nitrided austenitic stainless steel pre-treated with fine particle peening," *International Journal of Fatigue*, vol. 32, pp. 403-410, 2010.

[10] Y. Bai, M. Akita, Y. Uematsu, T. Kakiuchi, Y. Nakamura, and M. Nakajima, "Improvement of fatigue properties in type 304 stainless steel by annealing treatment in nitrogen gas," *Materials Science and Engineering: A*, vol. 607, pp. 578-588, 2014.

[11] M. Yasuoka, P. Wang, K. Zhang, Z. Qiu, K. Kusaka, Y.-S. Pyoun, *et al.*, "Improvement of the fatigue strength of SUS304 austenite stainless steel using ultrasonic nanocrystal surface modification," *Surface and Coatings Technology*, vol. 218, pp. 93-98, 2013.

[12] H. Stamm, U. Holzwarth, D. Boerman, F. Marques, A. Olchini, and R. Zausch, "Effect of laser surface treatment on high cycle fatigue of aisi 316L stainless steel," *Fatigue & Fracture of Engineering Materials & Structures*, vol. 19, pp. 985-995, 1996.

[13] Z. Wang, C. Jiang, X. Gan, Y. Chen, and V. Ji, "Influence of shot peening on the fatigue life of laser hardened 17-4PH steel," *International Journal of Fatigue*, vol. 33, pp. 549-556, 2011.

[14] D. Arola, A. Alade, and W. Weber, "Improving fatigue strength of metals using abrasive waterjet peening," *Machining science and technology*, vol. 10, pp. 197-218, 2006.

[15] T. Ogawa, S. E. Stanzl-Tschegg, and B. M. Schönbauer, "A fracture mechanics approach to interior fatigue crack growth in the very high cycle regime," *Engineering Fracture Mechanics*, vol. 115, pp. 241-254, 2014.

[16] J.-H. Wu and C.-K. Lin, "Effect of strain rate on high-temperature low-cycle fatigue of 17-4 PH stainless steels," *Materials Science and Engineering: A*, vol. 390, pp. 291-298, 2005.

[17] K.-C. Hsu and C.-K. Lin, "High-temperature fatigue crack growth behavior of 17-4 PH stainless steels," *Metallurgical and Materials Transactions A*, vol. 35, pp. 3018-3024, 2004.

[18] B. M. Schönbauer, K. Yanase, and M. Endo, "VHCF properties and fatigue limit prediction of precipitation hardened 17-4PH stainless steel," *International Journal of Fatigue*, vol. 88, pp. 205-216, 2016.

[19] J. Hao, S. Tang, H. Pan, and J. Chen, "Experimental study of fatigue crack growth rates of 17-4PH, 1Cr13 and 2Cr13 in air and chloride conditions," *Journal of Pressure Equipment and Systems*, vol. 3, pp. 157-161, 2005.

[20] J. Y. Kim, J. H. Lee, and S. H. Nahm, "Statistical Analysis of Casting Defects in Microstructure for Understanding the Effect on Fatigue Property of 17-4PH Stainless Steel," in *Key Engineering Materials*, 2006, pp. 1503-1506.

[21] B. M. Schönbauer, S. E. Stanzl-Tschegg, A. Perlega, R. N. Salzman, N. F. Rieger, A. Turnbull, *et al.*, "The influence of corrosion pits on the fatigue life of 17-4PH steam turbine blade steel," *Engineering Fracture Mechanics*, vol. 147, pp. 158-175, 2015.

[22] Z. LI and Z. CHEN, "Study on Fatigue Resistance of 17-4PH Stainless Steel After Laser Transformation Hardened [J]," *Hot Working Technology*, vol. 4, p. 062, 2013.

[23] P. Kochmański and J. Nowacki, "Activated gas nitriding of 17-4 PH stainless steel," *Surface and Coatings Technology*, vol. 200, pp. 6558-6562, 2006.

[24] Y. Li, L. Wang, J. Xu, and D. Zhang, "Plasma nitriding of AISI 316L austenitic stainless steels at anodic potential," *Surface and Coatings Technology*, vol. 206, pp. 2430-2437, 2012.

[25] R. Liu and M. Yan, "The microstructure and properties of 17-4PH martensitic precipitation hardening stainless steel modified by plasma nitrocarburizing," *Surface and Coatings Technology,* vol. 204, pp. 2251-2256, 2010.

[26] R. Liu, M. Yan, Y. Wu, and C. Zhao, "Microstructure and properties of 17-4PH steel plasma nitrocarburized with a carrier gas containing rare earth elements," *Materials Characterization,* vol. 61, pp. 19-24, 2010.

[27] D. Manova, G. Thorwarth, S. Mändl, H. Neumann, B. Stritzker, and B. Rauschenbach, "Variable lattice expansion in martensitic stainless steel after nitrogen ion implantation," *Nuclear Instruments and Methods in Physics Research Section B: Beam Interactions with Materials and Atoms,* vol. 242, pp. 285-288, 2006.

[28] T.-S. Shih, Y.-S. Huang, and C.-F. Chen, "Constituted oxides/nitrides on nitriding 304, 430 and 17-4 PH stainless steel in salt baths over the temperature range 723 to 923K," *Applied Surface Science,* vol. 258, pp. 81-88, 2011.

[29] F. Yıldız, A. Yetim, A. Alsaran, A. Çelik, and I. Kaymaz, "Fretting fatigue properties of plasma nitrided AISI 316L stainless steel: Experiments and finite element analysis," *Tribology International,* vol. 44, pp. 1979-1986, 2011.

[30] M. Yan, R. Liu, and D. Wu, "Improving the mechanical properties of 17-4PH stainless steel by low temperature plasma surface treatment," *Materials & Design,* vol. 31, pp. 2270-2273, 2010.

[31] T. Bell and N. Loh, "The fatigue characteristics of plasma nitrided three pct Cr-Mo steel," *Journal of Heat Treating,* vol. 2, pp. 232-237, 1982.

[32] M. Rahman, J. Haider, and M. Hashmi, "Low temperature plasma nitriding of 316 stainless steel by a saddle field fast atom beam source," *Surface and Coatings Technology,* vol. 200, pp. 1645-1651, 2005.

[33] S. P. Brühl, R. Charadia, S. Simison, D. G. Lamas, and A. Cabo, "Corrosion behavior of martensitic and precipitation hardening stainless steels treated by plasma nitriding," *Surface and Coatings Technology,* vol. 204, pp. 3280-3286, 2010.

[34] D. C. Wen, "Microstructure and corrosion resistance of the layers formed on the surface of precipitation hardenable plastic mold steel by plasma-nitriding," *Applied Surface Science,* vol. 256, pp. 797-804, 2009.

[35] D.-C. Wen, "Plasma nitriding of plastic mold steel to increase wear-and corrosion properties," *Surface and Coatings Technology,* vol. 204, pp. 511-519, 2009.

[36] Y. Xi, D. Liu, D. Han, and Z. Han, "Improvement of mechanical properties of martensitic stainless steel by plasma nitriding at low temperature," *Acta Metallurgica Sinica (English Letters),* vol. 21, pp. 21-29, 2008.

[37] L. Poirier, Y. Corre, and J. Lebrun, "Solutions to improve surface hardness of stainless steels without loss of corrosion resistance," *Surface engineering,* vol. 18, pp. 439-441, 2002.

[38] F. Haftlang, A. Habibolahzadeh, and M. H. Sohi, "Comparative tribological studies of duplex surface treated AISI 1045 steels fabricated by combinations of plasma nitriding and aluminizing," *Materials & Design,* vol. 60, pp. 580-586, 2014.

[39] I. VVAA, "1143: 2010,"Metallic materials–Rotating bar bending fatigue tests"," *International Organization of Standardization,* 2010.

[40] M. Takemura, T. Magai, and S. Yoshino, "17Cr-4 Ni-4Cu Precipitation Hardening Stainless Steel (The Third Report): The Carbide Reaction in the Tempering Process of

17Cr-4 Ni-4Cu-0.07 C Steel," *Annals of science the College of Liberal Arts, Kanazawa University*, vol. 4, pp. 1-14, 1968.

[41] M. Takemura, I. Shinoda, K. Kikuchi, and S. Yoshino, "17Cr-4Ni-4Cu Precipitation Hardening Stainless Steel (The Second Report): The Effect Additional Alloying Element (Ti, Mo, Al) on The Properties of The Cast Material," *Annals of science the College of Liberal Arts, Kanazawa University*, vol. 3, pp. 53-66, 1967.

[42] R. Bhambroo, S. Roychowdhury, V. Kain, and V. Raja, "Effect of reverted austenite on mechanical properties of precipitation hardenable 17-4 stainlesssteel," *Materials Science and Engineering: A*, vol. 568, pp. 127-133, 2013.

[43] B. L. Bramfitt and A. O. Benscoter, "Metallographer's guide," *Practices and Procedures for Irons and Steels, ASM International, Materials Park, OH, USA*, vol. 87, p. 3, 2002.

[44] M. Fitzpatrick, A. Fry, P. Holdway, F. Kandil, J. Shackleton, and L. Suominen, "Determination of residual stresses by X-ray diffraction," 2005.

[45] H. Dong, M. Esfandiari, and X. Li, "On the microstructure and phase identification of plasma nitrided 17-4PH precipitation hardening stainless steel," *Surface and Coatings Technology*, vol. 202, pp. 2969-2975, 2008.

[46] S. G. S. Raman and M. Jayaprakash, "Influence of plasma nitriding on plain fatigue and fretting fatigue behaviour of AISI 304 austenitic stainless steel," *Surface and Coatings Technology*, vol. 201, pp. 5906-5911, 2007.

[47] J. Wang, Y. Lin, M. Li, H. Fan, D. Zeng, and J. Xiong, "Effects of the Treating Time on Microstructure and Erosion Corrosion Behavior of Salt-Bath-Nitrided 17-4PH Stainless Steel," *Metallurgical and Materials Transactions B*, vol. 44, pp. 1010-1016, 2013.

[48] S. Grigull and S. Parascandola, "Ion-nitriding induced plastic deformation in austenitic stainless steel," *Journal of Applied Physics*, vol. 88, pp. 6925-6927, 2000.

[49] J. Stinville, P. Villechaise, C. Templier, J. Riviere, and M. Drouet, "Plasma nitriding of 316L austenitic stainless steel: Experimental investigation of fatigue life and surface evolution," *Surface and Coatings Technology*, vol. 204, pp. 1947-1951, 2010.

[50] W. Liang, "Surface modification of AISI 304 austenitic stainless steel by plasma nitriding," *Applied Surface Science*, vol. 211, pp. 308-314, 2003.